Basin Research

IAS EAGE

Basin Research (2017) 1–17, doi: 10.1111/bre.12270

A prograding margin during global sea-level maxima: an example from Mahajanga Basin, northwest Madagascar

Jonathan Obrist-Farner,*,[1] Philip J. Ball,*,†,[2] Thomas A. (Mac) McGilvery‡ and Raymond R. Rogers§

*ConocoPhillips Company, Houston, USA
†Geography, Geology and the Environment, Keele University, Newcastle, UK
‡Department of Geosciences, University of Arkansas, Fayetteville, AR, USA
§Geology Department, Macalester College, Saint Paul, MN, USA

ABSTRACT

The Mesozoic shelf margin in the Mahajanga Basin, northwest Madagascar, provides an example where inherited palaeobathymetry, coupled with sea-level changes, high sediment supply and fluctuations in accommodation influenced the stacking patterns and geometry of clinoforms that accreted onto a passive rifted margin. Two-dimensional (2D) seismic profiles are integrated with existing field data and geological maps to study the evolution of the margin. The basin contains complete records of transgression, highstand, regression and lowstand phases that took place from Jurassic to Cretaceous. Of particular interest is the Cretaceous, Albian to Turonian (*ca*. 113–93 Ma), siliciclastic shelf margin that prograded above a drowned Middle Jurassic carbonate platform. The siliciclastic phase of the shelf margin advanced *ca*. 70 km within *ca*. 20 My, and contains 10 distinct clinoforms mapped along a 2D seismic reflection data set. The clinoforms show a progressive decrease in height and slope length, and a fairly constant slope gradient through time. The successive shelf edges begin with a persistent flat to slightly downward-directed shelf-edge trajectory that changes to an ascending trajectory at the end of clinoform progradation. The progressive decrease in clinoform height and slope length is attributed to a decrease in accommodation. The prograding margin is interpreted to have formed when siliciclastic input increased as eastern Madagascar was uplifted. This work highlights the importance of sediment supply and inherited palaeobathymetry as controls on the evolution of shelf margins and it provides a new understanding of the evolution of the Mahajanga Basin during the Mesozoic.

INTRODUCTION

Clinoform progradation through time is one of the primary processes by which basin margins grow. Clinoform evolution and the sedimentary processes responsible for their trajectories and growth have been studied extensively (e.g. Posamentier & Vail, 1988; Pirmez *et al.*, 1998; Steckler *et al.*, 1999; Steel & Olsen, 2002; Johannessen & Steel, 2005; Kertznus & Kneller, 2009), and can be used to reconstruct the tectonic and sedimentary history of basin margins and to predict facies and facies distributions in the basin. Hence, there is significant scientific and economic interest in understanding the underlying controls on clinoform development.

Early sequence stratigraphic interpretations were based on the hypothesis that variations in clinoform geometries were due to changes in accommodation (e.g. Posamentier & Vail, 1988; Posamentier *et al.*, 1988). Current models, however, accept that it is difficult to reconstruct the history of a basin margin solely with the premise that changes in accommodation driven by eustatic sea-level control the stacking pattern of large-scale clinoforms. Rather, it is now understood that clinoform progradation and their resultant geometries during shelf-margin accretion are controlled by the complex interplay of tectonic movement, eustatic sea-level changes, basin physiography, sediment supply, sediment grain size and erosional processes that can modify the outer edges of the platform (Posamentier & Vail, 1988; Pirmez *et al.*, 1998; Steckler

Correspondence: Jonathan Obrist-Farner, Department of Geosciences, and Geological and Petroleum Engineering, Missouri University of Science and Technology, Rolla, MO 65409, USA. E-mail: obristj@mst.edu.
[1]Present address: Department of Geosciences, and Geological and Petroleum Engineering, Missouri University of Science and Technology, Rolla, MO 65409, USA
[2]Present address: Red Sea Exploration Department, Saudi Aramco, Dhahran 31311, Kingdom of Saudi Arabia

et al., 1999; Steel & Olsen, 2002; Kertznus & Kneller, 2009). Trajectory analysis is a method that has been used to decipher these processes (Helland-Hansen & Martinsen, 1996; Johannessen & Steel, 2005). For example, trajectories have been used to reflect changes in relative sea level (e.g. Muto & Steel, 2002) with flat or descending trajectories indicating a decrease and ascending trajectories an increase in relative sea level (Johannessen & Steel, 2005; Helland-Hansen & Hampson, 2009; Burgess & Prince, 2015). Other studies have showed that this inferred relationship of clinoform progradation and eustatic sea-level changes is not always clear and can be complicated by changes in accommodation, sediment supply, basin physiography and along strike variability in basin configuration (e.g. Henriksen *et al.*, 2011; Prince & Burgess, 2013; Burgess & Prince, 2015; Anell & Midtkandal, 2017).

This study evaluates the evolution of the Mahajanga Basin, NW Madagascar (Figs 1 and 2) with the purpose of (1) providing a robust stratigraphic framework for the onshore portion of the basin using 2D seismic profiles and previously published field maps and geological reports and (2) improving the understanding of the sedimentary succession in the Mahajanga Basin focusing on the Albian to Turonian prograding siliciclastic shelf margin.

The Cretaceous evolution of the basin margin, as evident from 2D seismic reflection profiles, was significantly influenced by eustatic fluctuations, basin physiography and by the breakup of eastern Gondwana. From Albian to Turonian (*ca.* 113-93 Ma), a siliciclastic margin prograded above a drowned Middle Jurassic carbonate platform that substantially controlled accommodation during progradation. The progradational sequence is characterized by sigmoidal and oblique/tangential clinoforms (Mitchum *et al.*, 1977). Successive clinoform mapping illustrates the basinward migration of the Mahajanga Basin margin throughout much of the Mesozoic. Clinoform height and slope length decrease through time and display a flat to slightly downward-directed shelf-edge trajectory with clear tangential oblique clinoforms. The trajectory and clinoform geometry change at the end Turonian to ascending and sigmoidal, respectively,

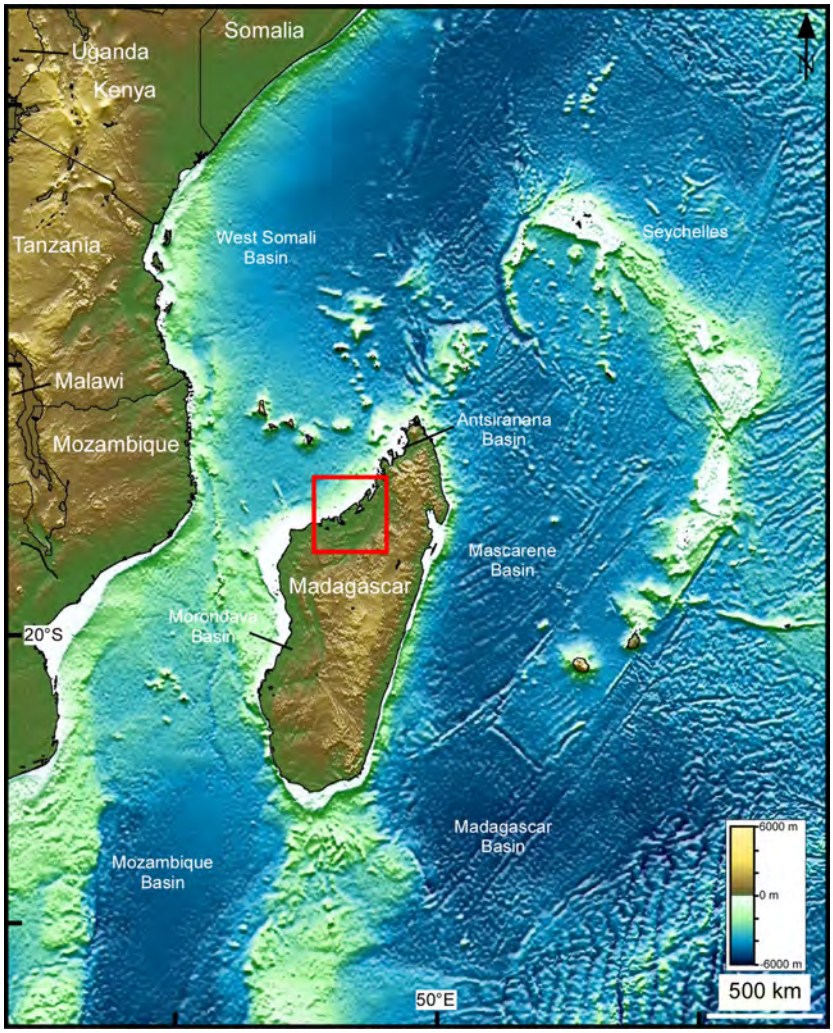

Fig. 1. Topographic relief map of eastern Africa with the location of major basins. Red box highlights the location of the study area within the Mahajanga Basin in northwest Madagascar.

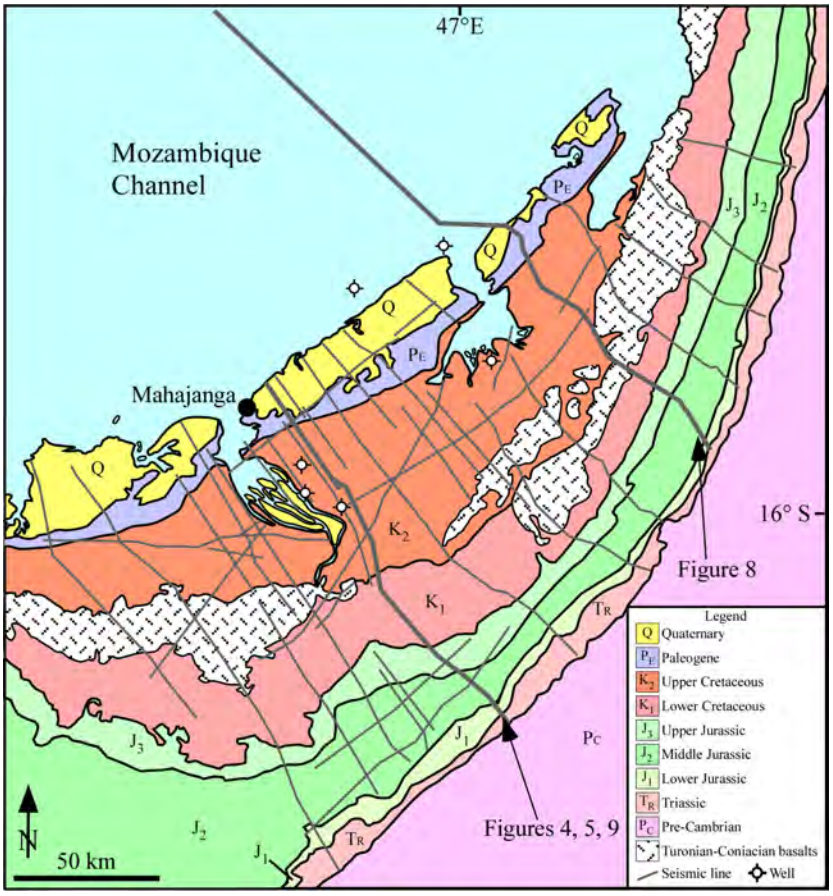

Fig. 2. Geological map of the Mahajanga Basin, northwest Madagascar with location of 2D seismic profiles used in this study. Geological map is highly modified from Roig *et al.* (2012). See Figure 1 for location of study area.

accompanied by a decrease in clinoform height and slope length driven by a systematic decrease in accommodation. The trajectory of the shelf edge is interpreted as the result of a constant and high supply of sediment sourced from the uplifted eastern margin of Madagascar and the geometrical characteristics of the clinoforms are interpreted to have been influenced by sediment supply and basin physiography. This study sheds light on processes and factors controlling shelf-margin accretion and provides an example from an understudied basin in East Africa.

GEOLOGICAL SETTING

Tectonic background

The Mahajanga Basin evolved into a passive margin after the successful localization of rifting processes and the initiation of seafloor spreading in the West Somali Basin with chron M40ny, at *ca*. 170 Ma (Gaina *et al.*, 2013). The breakup event followed discrete rifting events that started as early as the Permian in Gondwana (Schandelmeier *et al.*, 2004; Leinweber & Jokat, 2012). The West Somali Basin appears to have transitioned to seafloor spreading simultaneously or just after spreading initiated within the Mozambique Basin to the south (Eagles & König, 2008; Nguyen *et al.*, 2016). The breakup event began with a NNW-SSE plate motion between Africa and eastern Gondwana, which was composed of Madagascar, Seychelles, India, Antarctica and Australia (Eagles & König, 2008; Gaina *et al.*, 2013, 2015; Nguyen *et al.*, 2016; Reeves *et al.*, 2016). The motion of Madagascar from East Africa changed to a more N-S drift at *ca*. 140 Ma (Gaina *et al.*, 2013). Seafloor spreading in the West Somali Basin slowed from *ca*. 132 Ma and ceased at *ca*. 123 Ma, coinciding with stress changes in plate boundaries between Madagascar, India, Australia and Antarctica (Gaina *et al.*, 2013, 2015). As spreading halted in the West Somali Basin, the plate boundary relocated to the east, accommodating transpressional motion between India and Madagascar, responding to the breakup between India and Australia–Antarctica (Gibbons *et al.*, 2013; Gaina *et al.*, 2015). Strike-slip motion between Madagascar and India continued until *ca*. 88 Ma when spreading initiated in the Mascarene Basin between Madagascar and India–Seychelles (Gaina *et al.*, 2015). Breakup between India–Seychelles and Madagascar was also coeval with regional, possibly, Marion hot-spot related volcanism that is identified across Madagascar and India (Storey *et al.*, 1997; Torsvik *et al.*, 2000; Melluso *et al.*, 2001; Bardintzeff *et al.*, 2010; Cucciniello *et al.*, 2013). In the Mahajanga

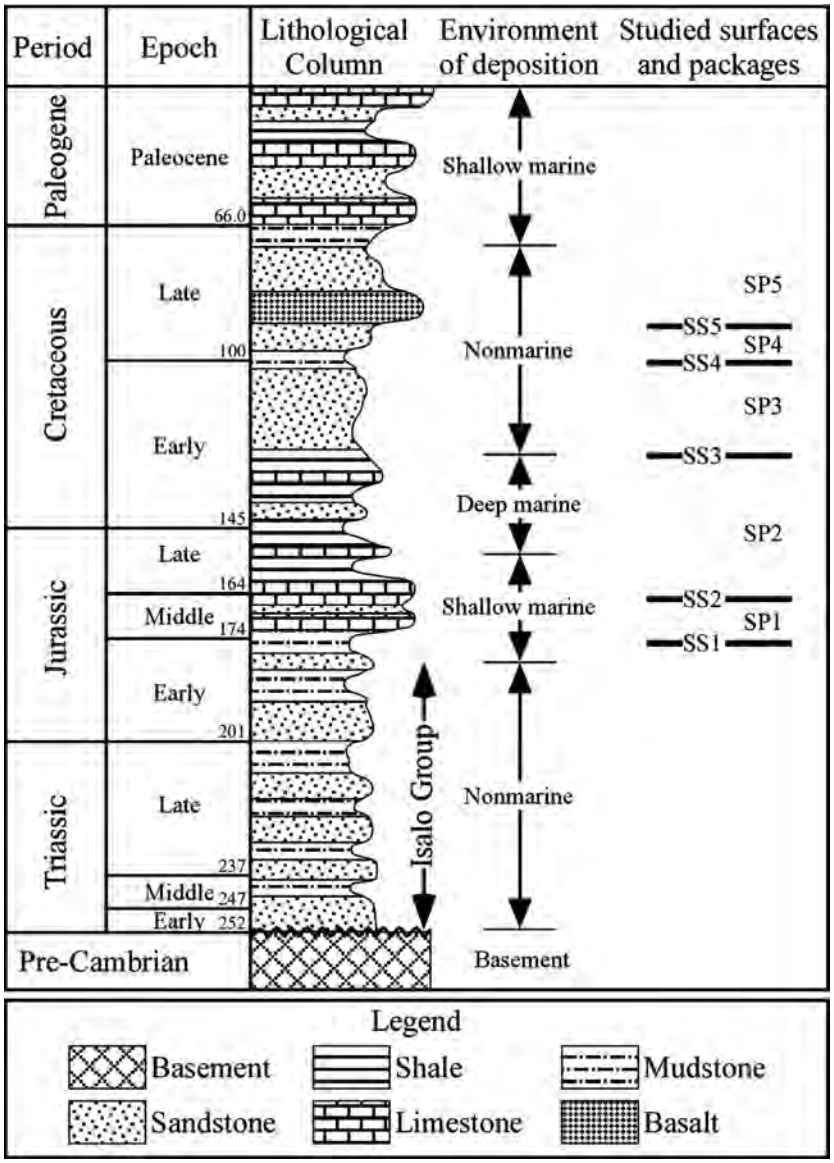

Fig. 3. Highly simplified stratigraphy and lithological column from Mahajanga Basin, NW Madagascar. Lithological column modified and simplified from Besairie (1972). Absolute ages at epoch boundaries from Gradstein *et al.* (2004). See Figure 4 and text for details on seismic surfaces and packages.

Basin, this volcanic activity culminated in *ca*. 200 m of Turonian to Coniacian (92–84 Ma) basalts (Besairie, 1972; Storey *et al.*, 1997; Torsvik *et al.*, 2000; Figs 2 and 3). Following the initiation of rifting processes (*ca*. 170 Ma) and subsequent demise of spreading within the West Somali Basin at *ca*. 123 Ma (Gaina *et al.*, 2013), the Mahajanga margin persisted as a passive margin and was slowly filled with marine and nonmarine deposits. The proximal rift margin deposits are exposed present day onshore (Figs 2 and 4). Early uplift and basin tilting events appear to be associated with evolving plate boundaries, as rifting and seafloor spreading relocated eastwards and transpressional processes occurred on the eastern margin of Madagascar at 130–125 Ma and *ca*. 120–88 Ma (e.g. Gaina *et al.*, 2013, 2015). This tilting was possibly amplified due to sedimentary loading and flexure within the Mahajanga and Morondava basins (Seward *et al.*, 2004; Emmel *et al.*, 2012), and also due to a modern-day reactivation of the hinterland due to the upwelling of the asthenosphere under central Madagascar (e.g. Roberts *et al.*, 2012; Pratt *et al.*, 2016).

Stratigraphy

Mesozoic and Paleogene strata are exposed and can be mapped in the outcrops of the Mahajanga Basin (Fig. 2). The basic stratigraphy and sedimentology of the entire succession was first documented by Besairie (1972), who provided a broad-ranging lithological and palaeontological overview of the succession. The expansive early work of Besairie (1972) set the stage for interpreting the depositional history of the Mahajanga Basin and provided a

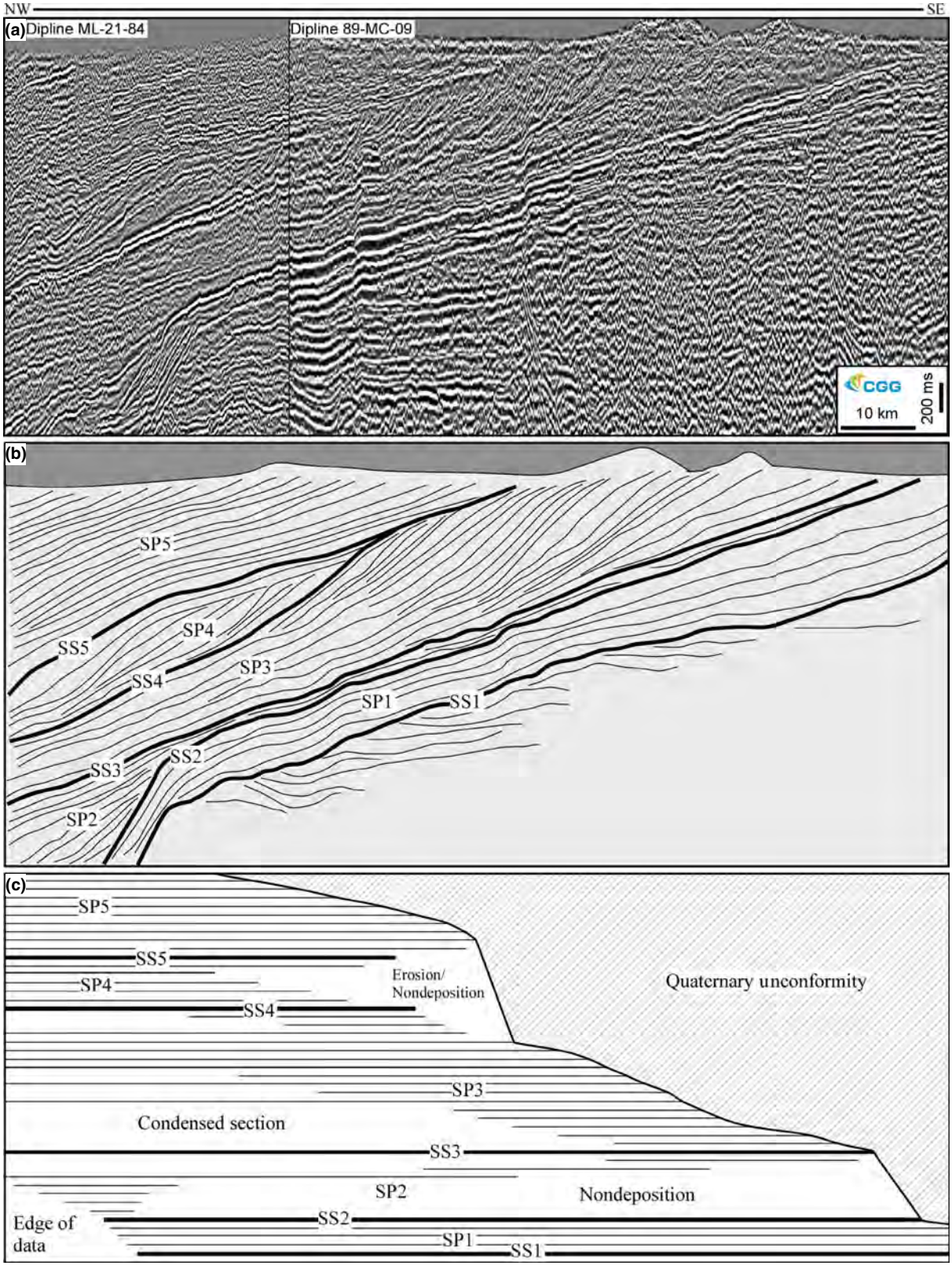

Fig. 4. (a) Uninterpreted seismic line from the Mahajanga Basin. (b) Interpreted schematic diagram of seismic line. Notice the exposure of sloping segments and topsets of clinoforms onshore Madagascar. Seismic surfaces and packages are described in the text. (c) Chronostratigraphic interpretation (Wheeler diagram) of seismic profile in 4a. See text for details. See Figure 2 for location of seismic line. Seismic line courtesy of OMNIS and CGG MCNV (GeoSpec).

regional stratigraphic framework across the basin using lithological and palaeontological data (Fig. 3). More recent studies have dealt specifically with improving the lithostratigraphy and chronostratigraphy of the basin fill (e.g. Papini & Benvenuti, 1998; Rogers *et al.*, 2000, 2013), but have focused mainly on Upper Cretaceous strata due to the presence of superbly preserved vertebrate fossils (e.g. Rogers, 2005; Rogers *et al.*, 2003, 2007, 2013). Even though much of the Triassic to Paleogene succession remains only generally described, an overall description of the stratigraphic succession is provided below using previously published data (e.g. Besairie, 1972; Luger *et al.*, 1994; Papini & Benvenuti, 1998, 2008; Rogers *et al.*, 2000, 2013; Abramovich *et al.*, 2002; Geiger *et al.*, 2004; Fig. 3).

The Upper Triassic–Lower Jurassic sedimentary succession is known as the Isalo Group and is characterized by continental sandstones interbedded with mudstones that vary in thickness from 10 to 100s of metres across the basin (Besairie, 1972; Fig. 3). The Isalo Group is informally subdivided into three units: Isalo I, II and III. In the Morondava Basin, Geiger *et al.* (2004; Fig. 1) suggest that the Isalo I and II are Triassic in age and the Isalo III Lower Jurassic. This subdivision helps constrain the age of strata in the Mahajanga Basin although the absolute ages of the Isalo units are uncertain. A gradual change from siliciclastic to carbonate deposition occurs during the Middle Jurassic in the Mahajanga Basin (Besairie, 1972), in the Morondava Basin to the south (Luger *et al.*, 1994; Geiger *et al.*, 2004; Fig. 1) and in the Antsiranana Basin to the north (Papini & Benvenuti, 2008; Fig. 1). Carbonate deposition became dominant during Callovian (Besairie, 1972) and an abundance of marine fossils indicates that widespread marine conditions were established in the basin. The Upper Jurassic sedimentary succession is characterized by 100 to *ca*. 200 m of shales and mudstones interbedded with beds of limestone, marl and sandstone, indicative of persistent marine conditions. Besairie (1972) noted a significant basinwide gap in deposition during the Late Jurassic that he attributed to a possible submarine erosional event. Shale deposition continued throughout the Early Cretaceous until the Aptian–Albian, during which up to 600 m of sandstone and conglomerate were deposited (Besairie, 1972), marking the transition from carbonate- to siliciclastic-dominated deposition. The thickest sandstone deposits are concentrated east of the city of Mahajanga (Fig. 2) and disappear in the northern and southern parts of the basin (Besairie, 1972). Besairie (1972) suggested that Aptian–Albian to Turonian deposits formed mainly in a continental environment, although he did recognize occasional marine tongues (Fig. 3). Turonian to Coniacian deposits are characterized by continental sandstones and mudstones and extruded basalts (Besairie, 1972; Storey *et al.*, 1997; Torsvik *et al.*, 2000; Fig. 3). Continental and shallow marine deposition continued until the end Cretaceous, with shallow marine conditions persisting in the Paleogene (Besairie, 1972; Papini & Benvenuti, 1998; Rogers *et al.*, 2000, 2013; Abramovich *et al.*, 2002).

DATA AND METHODOLOGY

Forty-one 2D onshore seismic reflection profiles are used in this study; twenty-eight are dip oriented, six are oblique oriented and seven are strike oriented (Fig. 2). A stratigraphic framework is developed using a published geologic map of the Mahajanga Basin (Roig *et al.*, 2012) and available palaeontological and stratigraphic data (e.g. Besairie, 1972). Proprietary well data near the seismic profile shown in Figure 4 and stratigraphic contacts mapped in outcrop provide a direct calibration and a reasonable framework for correlation and age constraint of mapped seismic horizons (Figs 2 and 5).

The sedimentary succession is subdivided into five seismic packages (SP) based on seismic characteristics (Fig. 4). Each package is separated by bounding surfaces (SS) that are defined on the basis of seismic amplitude and continuity as well as stratal termination patterns (Fig. 4). The top and bottom rollover points of clinoforms (e.g. Patruno *et al.*, 2015) are qualitatively interpreted and used to interpret compacted clinoform height, slope gradient and slope length (Fig. 6). Clinoform heights assume a 1 : 1 conversion between two-way travel time and depth. This conversion is in agreement with the thickness observed from the three wells near the seismic profile in Figure 4. The 1 : 1 conversion would assume a velocity of 2400 m s^{-1} for the sediments. This is an approximation designed to enable the comparison of the geometrical characteristics of the clinoforms in this study with those in other basin margins. Given the shallow depth of burial of the Albian–Turonian clinoforms, this time–depth approximation should not introduce a significant error. The same is not true below the Upper Jurassic shales, where the Middle Jurassic carbonate platform, Lower Jurassic to Triassic sediments and basement are likely to have significantly increased velocities.

Clinoform geometrical characteristics are calculated using the aforementioned time–depth conversion. Length is the distance between top and bottom rollover points of a clinoform and slope gradient is the angle between clinoform height and the distance between the two rollover points (Fig. 6). Successive top rollover points define the overall trajectory of the shelf edge (Fig. 6). These trajectories and the corresponding angle between rollover points are calculated by flattening the seismic line on a maximum flooding surface (SS3 – see below), which is the best candidate for a nearly horizontal marker (Helland-Hansen & Hampson, 2009).

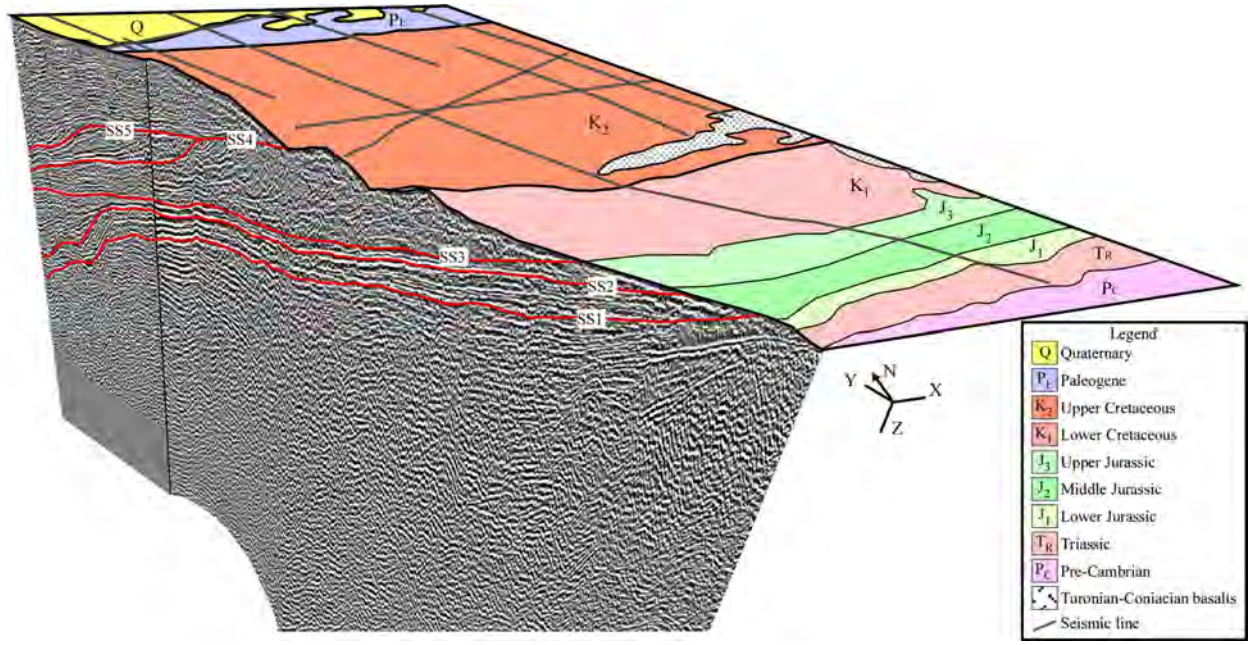

Fig. 5. Three-dimensional diagram displaying the methodology used to establish the chronology of seismic surfaces using the geological map of the Mahajanga Basin. See Figure 2 for location of seismic line. Seismic line courtesy of OMNIS and CGG MCNV (GeoSpec). Geological map is highly modified from Roig *et al.* (2012). Diagram not drawn to scale. See Figs. 2 and 4 for scale.

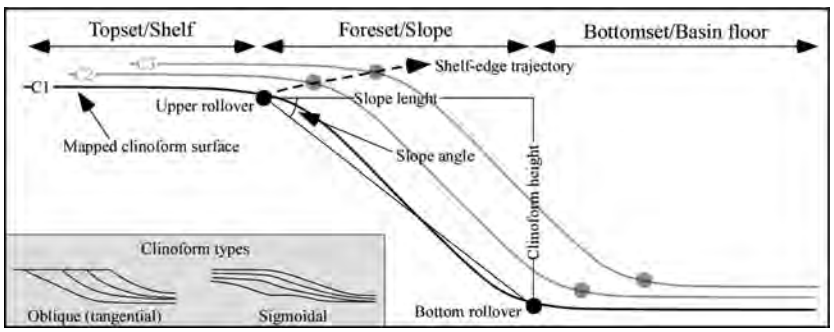

Fig. 6. Simplified cross-sectional schematic profile of a clinoform highlighting depositional provinces, geometries calculated in this study, and points of significant change in slope (rollover points). Modified from Helland-Hansen & Hampson (2009). Grey box contains a schematic profile of the two types of clinoforms recognized in this study. Modified from Mitchum *et al.* (1977).

OBSERVATIONS AND RESULTS

Seismic surfaces and packages

The sedimentary succession in the Mahajanga Basin is subdivided into five seismic packages (Fig. 4). These packages are described based on seismic facies (e.g. Mitchum *et al.*, 1977) and combined with outcrop data from Besairie (1972; Fig. 5) to interpret depositional environments and system tracts. Individual packages are separated by basinwide correlative seismic surfaces (Fig. 4). Seismic packages and their bounding surfaces represent significant changes in basin configuration, accommodation, sediment supply or tectonics. Seismic surfaces and their significance are described and later combined with seismic packages to describe the history of the basin fill.

Seismic surfaces

Seismic surface one (SS1) underlies seismic package 1 (SP1) and is characterized by a high-amplitude seismic reflection (Fig. 4). Clear truncation termination patterns are evident below SS1 and define an angular unconformity. Seismic reflections above SS1 are parallel to SS1. In the northwestern part of the data set, the surface is difficult to correlate due to poor image quality and edge of the

data set. SS1 is interpreted as the breakup unconformity between Madagascar and Africa and could be Bajocian in age (*ca*. 170 Ma) based on geological ages from the outcrops (Fig. 5), magnetic isochron interpretations (e.g. Gaina *et al.*, 2013) and similar observations from the southern Morondava Basin (e.g. Geiger *et al.*, 2004).

SS2 overlies SP1 and underlies SP2 and is easily correlated due to its high amplitude and continuity (Fig. 4). The surface is flat in the southeastern part, but changes to a dipping surface marking the point of maximum progradation of SP1 in the northwestern part of the data set. Seismic horizons below the surface are parallel to SS2. Those above are parallel and exhibit a low-angle onlap termination pattern in the southeastern side of the data set. High angle onlap termination patterns are clear in the northwestern side of the data set against the dipping segment of the surface. SS2 is interpreted as a maximum regressive surface (Catuneanu, 2002) due to a slightly progradational SP1 below (see description below) and onlapping termination patterns above. The surface is interpreted as Middle Jurassic based on the seismic tie with outcrop data (Fig. 5).

SS3 overlies SP2 across a conformable and flat surface (Fig. 4). SP3, however, downlaps onto SS3 in the southeastern parts of the data set and changes to a parallel surface in the northwestern part of the data set. SS3 is a low-amplitude horizon, but it is continuous across the basin. It is interpreted as a maximum flooding surface (Posamentier *et al.*, 1988) because of the downlapping surfaces above. The surface is interpreted as Late Jurassic–Early Cretaceous based on the seismic tie with outcrop data (Fig. 5).

SS4 is a high-amplitude surface that separates SP3 and SP4 (Fig. 4). The surface is flat in the southeastern part and slightly dips in the northwestern part of the data set. Surfaces below display a truncation/toplap termination pattern; surfaces above are parallel and in some cases display an onlap termination pattern. SS4 is interpreted as a subaerial unconformity in its southeastern extent and a correlative conformity in the northwestern part of the data set and is of Albian–Cenomanian age (Fig. 5).

SS5 separates SP4 and SP5 across a conformable surface (Fig. 4). The surface has a low amplitude and is continuous across the data set. The surface is flat with a slight dip in the northwestern side of the data set. SS5 onlaps onto SP4 in the southeastern part of the data set. SS5 is interpreted as a maximum regressive surface (Catuneanu, 2002) of Turonian age (Fig. 5) separating lowstand deposits below and transgressive deposits above.

Seismic packages

The sedimentary interval below SP1 is difficult to describe with the current data set. Previous studies in the Mahajanga and Morondava basins have shown that the basement and sedimentary package below the carbonate platform include tilted, distorted and highly discontinuous seismic horizons. The sedimentary fill appears to have been deposited in small grabens and half grabens surrounded by rotated basement blocks and horsts (e.g. Luger *et al.*, 1994; Geiger *et al.*, 2004; Tari *et al.*, 2004; Giese *et al.*, 2012; Figs 4 and 8). The sedimentary fill is interpreted to be age equivalent to the Late Triassic to Early Jurassic fluvial and lacustrine deposits that accumulated in grabens and half grabens as rifting between Africa and Madagascar began (Besairie, 1972).

SP1 unconformably overlies the Late Triassic–Early Jurassic sedimentary fill across SS1 and underlies SS2 across a conformable surface. SP1 is characterized by high-amplitude and parallel seismic reflections. The package displays a typical rimmed platform morphology (e.g. Pomar, 2001; Fig. 4) that is aggradational from SS1 to SS2. SP1 has a clear shelf to slope break and is interpreted as a Middle Jurassic carbonate platform based on the tie to outcrop observations to the southeast made by Besairie (1972; Fig. 5). The lower part of the package may correlate to the first marine incursion in the Mahajanga Basin and represents a change from a siliciclastic- to a carbonate-dominated margin. Mapping of the SS2 shelf/slope break reveals a westward-facing convex shelf-edge morphology across the basin (Fig. 7). The geometrical characteristics of the clinoforms in SP1 are uncertain because seismic data seaward of the shelf edge is of poor

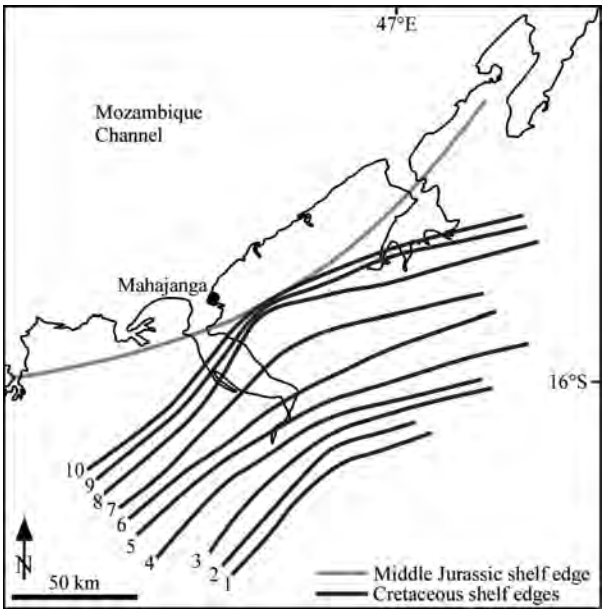

Fig. 7. Map of the Mahajanga Basin with the interpreted Middle Jurassic and Albian–Turonian shelf edges. The Middle Jurassic shelf edge is characterized by a westward facing convex morphology, while the prograding Albian–Turonian shelf edges are concave. Shelf-edge numbers correspond to the same numbered clinoforms in Fig. 9.

quality and the bottomsets are not well imaged (Fig. 4). The relief from shelf to basin floor, however, appears to be significant (e.g. Tari *et al.*, 2004; Fig. 8).

SP2 overlies SP1 across a conformable parallel surface (SS2) and underlies SP3 across a conformable downlapping surface (SS3). SP2 is thick in the northwestern part of the data set where it onlaps SS2 basinward of the Middle Jurassic shelf edge. The package thins elsewhere and is parallel to SS2 landward of the Middle Jurassic shelf edge. The package is interpreted to represent a lowstand to transgressive/flooding event that is Late Jurassic–Early Cretaceous in age with a capping maximum flooding surface (SS3). The onlap surfaces on the northwestern part of the data set define the maximum progradation of SP1. These onlapping surfaces could be talus deposits from the previous Middle Jurassic carbonate shelf (SP1) or it could record deposition in a starved setting as the carbonate platform was flooded and the carbonate factory shut down. In outcrop, Besairie (1972) noted a change to shale- and mudstone-dominated deposition with abundant pyrite, anhydrite and glauconite which could have been deposited in deep water settings.

SP3 downlaps onto SS3 in the southeastern part of the data set and progressively becomes parallel to SS3 on the northwestern side of the data set (Fig. 4). SP3 is characterized by at least six well-developed clinoforms that are complete (topset, foreset, bottomset; Fig. 6) and mappable across the entire data set. The clinoforms are mainly tangential oblique (Mitchum *et al.*, 1977) but vary along the data set between sigmoidal and tangential oblique (Fig. 6). The progradational package is interpreted as Albian to Cenomanian highstand deposits (*ca.* 113-99.6 Ma). In outcrop, Besairie (1972) noted an up to 360-m-thick sandstone unit (Sandstone of Ankarafantsika; Besairie, 1972) east of the city of Mahajanga that he interpreted as possible deltaic or beach/shoreface deposits.

SP4 overlies SP3 across an unconformity and correlative conformity. It is characterized by four clinoforms that are complete and commonly display dipping surfaces within mapped clinoforms. The clinoforms are sigmoidal in a single 2D profile but change laterally in geometry and size and disappear in the northern part of the basin (Fig. 6). The package is interpreted as a Cenomanian–Turonian lowstand wedge and represents the maximum regressive phase during the evolution of the margin. Turonian outcrops are characterized by 100- to 200-m-thick continental deposits that thin towards the southern and northern parts of the basin and are overlain by Turonian–Coniacian basalts (Besairie, 1972).

SP5 is characterized by parallel reflections that are continuous across the basin and display an onlap termination pattern onto SS5 and SS4. In some parts of the basin, the package contains highly distorted and chaotic reflections. The package is interpreted as transgressive and highstand topsets characterized by continental and shallow marine deposits (e.g. Besairie, 1972; Rogers *et al.*, 2000, 2013; Abramovich *et al.*, 2002). The chaotic packages on seismic lines appear to correspond to the location of basalts that were extruded during Turonian–Coniacian (92–84 Ma; Storey *et al.*, 1997; Torsvik *et al.*, 2000; Figs 2 and 3). These basalts are interbedded with shallow marine and continental deposits (Besairie, 1972), indicating an increase in sea level and subsequent flooding of the margin.

Clinoforms and clinoform geometries

Analysis of individual clinoforms within SP3 and SP4 allows for the interpretation of higher frequency changes throughout the succession. Clinoforms in SP3 and SP4 represent not only the sloping segment of the surface, but the entire sigmoid; topsets, foresets and bottomsets (e.g. Mitchum *et al.*, 1977; Steel & Olsen, 2002; cf. Rich, 1951; Fig. 6). Ten complete clinoforms are preserved within

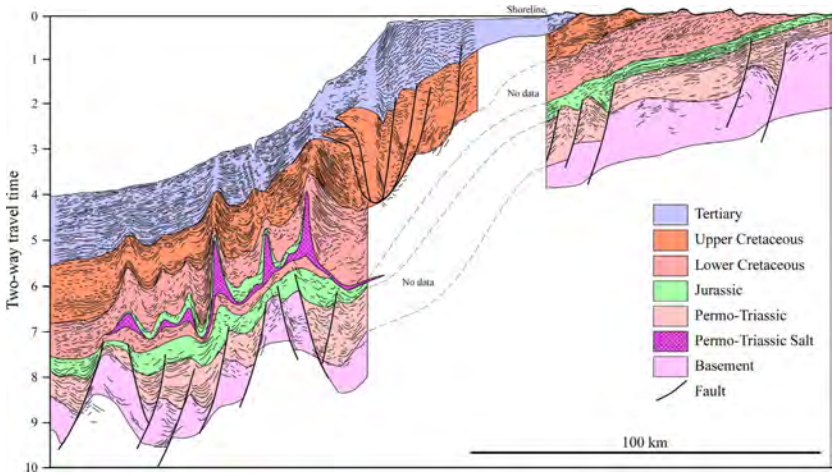

Fig. 8. Regional interpreted geoseismic transect across the northern part of the Mahajanga Basin with a vertical exaggeration of 4 km sec^{-1}. Modern shelf is a poor seismic data area. See Figure 2 for location of seismic line. Geoseismic transect provided by G. Tari. Modified from Tari *et al.* (2004).

SP3 and SP4 (six and four respectively). They vary from sigmoidal to tangential oblique in a single 2D profile (Figs 6 and 9). Additional clinoforms are observed on various 2D profiles but are difficult to correlate across the complete data set due to line spacing (*ca*. 25 km; Fig. 2) and quality (Fig. 4). Clinoform 1 (C1) through C6 are tangential oblique with toplap termination patterns (Fig. 9). C1 downlaps onto SS3, while C2 and C6 have well-developed bottomsets that are parallel to SS3 (Fig. 8). C7 through C10 change to sigmoidal clinoforms and contain longer topsets and shorter foresets (bottomsets are not observed due to edge of data).

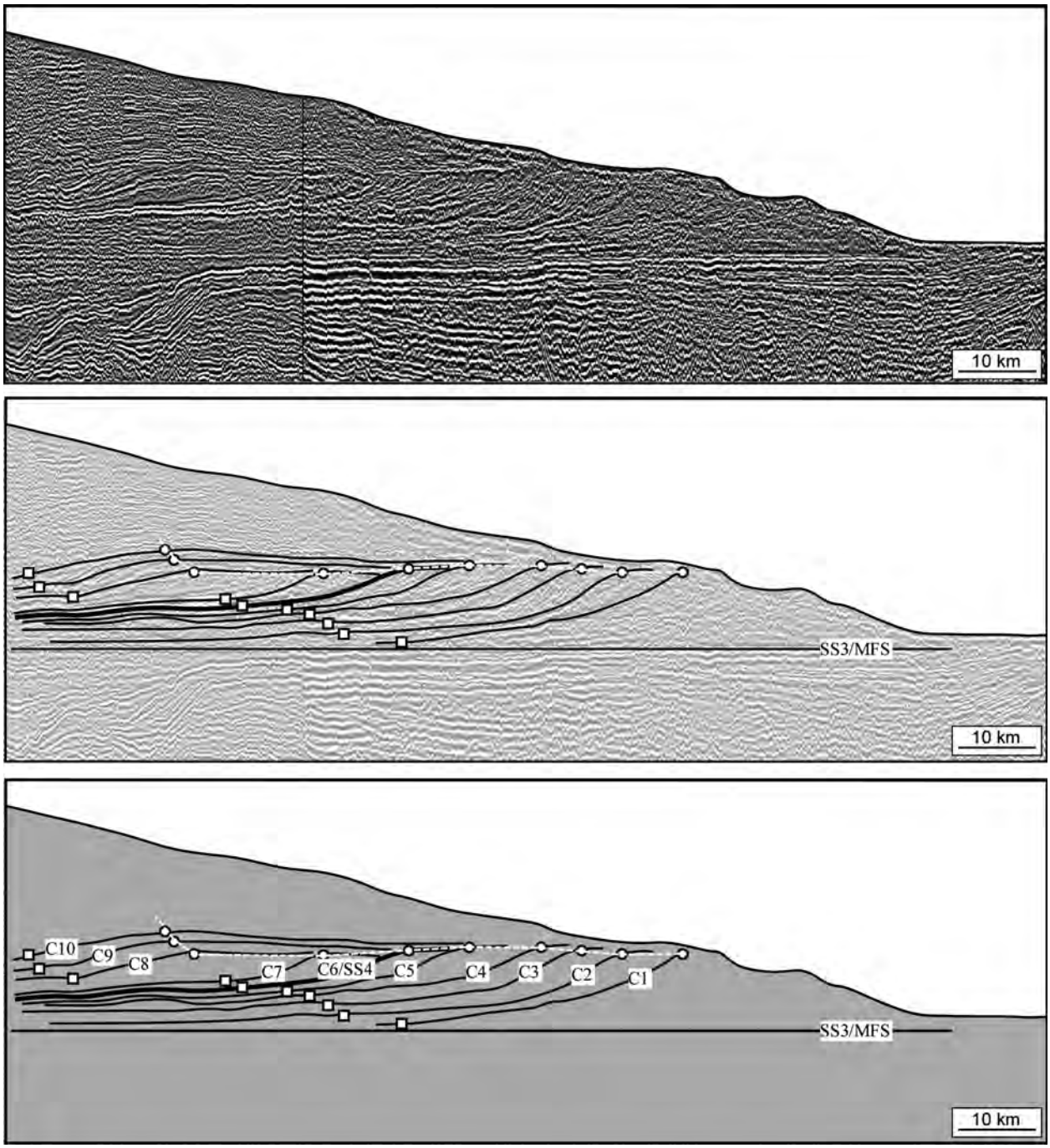

Fig. 9. Uninterpreted, interpreted and schematic diagram of clinoforms interpreted in this study. See Fig. 2 for line location. Seismic line is flattened on the maximum flooding surface (SS3). Notice the flat trajectory of C1 through C6, the change to a downward-directed trajectory from C6 to C8 and the change to an ascending trajectory from C8 to C10. Black and white circles mark the interpreted topset to foreset transition; white dashed line is the overall trajectory of the shelf edge. Black and white squares mark the interpreted foreset to bottomset transition.

The upper rollover points of C1 through C10 (topset to foreset transition; Fig. 6) define the individual shelf edges and can be correlated laterally along the basin. The results reveal a northwest-directed migration of the margin through time (Fig. 7). To the north of the data set, the upper rollover point is difficult to interpret due to a change in clinoform geometry from sigmoidal/tangential oblique to a ramp-like morphology. Therefore, the exact location of the shelf edge is uncertain and not mapped (Fig. 7).

Geometrical analysis of the 10 clinoforms along a single profile (Fig. 9) assuming a 1 : 1 conversion between two-way travel time and depth indicates: (1) a fairly constant slope gradient between 0.7° and 1.0° for all clinoforms, (2) a progressive reduction in clinoform height from 588 m (C1) to 293 m (C10) and (3) a progressive decrease in slope length from *ca*. 45 km (C1) to *ca*. 15 km (C10; Table 1). An average progradational rate for all clinoforms is calculated assuming a constant rate of progradation. The results indicate an approximate rate of *ca*. 3 km My^{-1} for *ca*. 70 km. This calculation is possibly an underestimation because it is considerably smaller than published progradational rates of clinoforms in other settings with better chronological constraints (Table 1). Nevertheless, it offers a rough estimate of the timing and pace at which the clinoforms evolved.

The clinoforms in this study are interpreted as shelf-margin clinoforms due to their size and geometrical characteristics (e.g. Steel & Olsen, 2002; Helland-Hansen & Hampson, 2009). The dominance of tangential oblique clinoforms from C1 through C6 suggests a relatively high sediment supply with minimal creation of accommodation and some degree of bypass and erosion in a coastal plain environment. The majority of the sediment budget probably was spent building the basinward stepping slope clinoforms. The infill of the basin and the highly progradational margin suggests a eustatic stillstand in sea level that allowed rapid infill and sediment bypass on the upper C1 through C6 surface. The topsets of C1 through C3 are exposed in outcrop (Figs 4,5,7) and contain abundant sandstone and conglomerate deposits, indicating an increase in siliciclastic input into the basin (Besairie, 1972). The transition to sigmoidal clinoforms from C7 through C10 indicates a change in basin configuration, sea level and/or sediment supply. C7 and C8 are interpreted as lowstand deposits defined by topset bypass across SS4 with minimal accommodation due to their significant reduction in clinoform height with a bypass composite topset surface separating C7 and C8 from C9. On the other hand, C9 and C10 contain aggrading topsets that suggest accommodation creation with a turnaround in relative sea level (Fig. 9). This interpretation is supported by the onlapping deposits of SP5 above C10, consistent with transgression.

Table 1. Clinoform geometries from modern and ancient shelf margins

Location	Age	Basin type	Data	Clinoform	Slope		Rate of progradation (km My^{-1})	References
				Height (m)	Length (km)	Gradient (°)		
Mahajanga Basin, Madagascar	Albian–Turonian	Post-rift passive margin	2D seismic	270–588	15–45	0.7–1	*ca*. 3	This study
Porcupine Basin, Ireland	Eocene	Post-rift passive margin	3D seismic	250–300	6–7	2–3	–	Johannessen & Steel (2005)
New Jersey, USA	Eocene–Miocene	Post-rift passive margin	2D seismic	22–257	–	*ca*. 1–2.7	–	Steckler *et al*. (1999)
Ebro margin, Spain	Plio-Pleistocene	Post-rift passive margin	3D seismic	145–1800	–	1–8	6.8–11.4	Kertznus & Kneller (2009)
Spitsbergen, Norway	Eocene	Foreland basin	Outcrop	250–350	<5	3–4	–	Steel & Olsen (2002)
Wyoming, USA	Maastrichtian	Foreland basin	Well	*ca*. 430	–	–	47.8	Carvajal & Steel (2006)
Karoo Basin, South Africa	Permian	Foreland basin	Outcrop	200	22	0.5	–	Wild *et al*. (2009)
Magallanes Basin, Chile	Cretaceous–Paleogene	Foreland basin	Outcrop	740–870	23–30	1.7–1.8	–	Hubbard *et al*. (2010)

Trajectory analysis

Successive mapping of the shelf edge in a single 2D profile reveals three distinct trajectories in the Cretaceous between *ca*. 113 and 93 Ma. These trajectories are calculated on a 2D profile flattened along the SS3 maximum flooding surface (Fig. 9). The first six clinoforms (C1–C6) have a flat to slightly downward-directed trajectory (Fig. 9). These clinoforms prograded *ca*. 40 km which accounts for approximately half of the total progradation of the margin. The dip-plane between successive top rollover points along the first six clinoforms is fairly constant, ranging between 0.16° and 0.34°. This shallow angle defines a composite topset surface for all six clinoforms that is highly progradational with no topset aggradation. C7 and C8 record a basinward shift with a significant amount of bypass/erosion indicated by the truncation/toplap at the top C7 clinoform. This basinward shift is indicated by onlap of the C7 surface at a downward step of −0.08° below the C6 rollover point (SS4; Figs 4 and 9). Clinoforms C7 and C8 prograded for *ca*. 30 km and their trajectory is nearly flat at 0.04°. These two clinoforms are interpreted as a gross lowstand interval. The clinoforms above C8 record a turnaround and transition to an upward deepening, transgressive succession. Progradation decreases to *ca*. 2.6 km during this time and their trajectories change to ascending with a positive trajectory angle of 1.2° and 3.0° between C8 and C9 and between C9 and C10 respectively. Above C10, onlapping transgressive deposits are observed and are interpreted as a flooding event and a backstep of the margin.

DISCUSSION

An understanding of the processes and mechanisms controlling the Middle Jurassic to Late Cretaceous margin evolution of the Mahajanga Basin has been developed. The evolution of the margin can be subdivided into five stages (Fig. 4): (1) a Middle Jurassic unconformity related to the breakup between Africa and Madagascar (SS1); (2) the establishment of a Middle Jurassic carbonate platform (SP1 and SS2); (3) a transgressive drowning event during Late Jurassic-Early Cretaceous (SS3); (4) a highly progradational siliciclastic shelf margin during Early- and Late-Cretaceous (SP3 and SP4) and (5) a transgressive, aggradational margin during Latest Cretaceous (SP5).

The siliciclastic Albian–Turonian (113-93 Ma) prograding margin in Madagascar (SP3-SP4) appears to have resulted from the interplay between palaeobathymetry, sea level, hinterland uplift and resultant increase in sediment supply and climate. During the progradational phase of the margin, global sea level was at the highest level of the Phanerozoic (Schlanger *et al.*, 1987; Miller *et al.*, 2005). The persistence of tangential oblique clinoforms (Fig. 9) indicates a stillstand in sea level (e.g. Mitchum *et al.*, 1977; Vail & Mitchum, 1977) in the Mahajanga Basin. During this time, the margin may be characterized as 'low accommodation supply driven' thus becoming highly progradational (e.g. Goodbreed & Kuehl, 2000) with minimal topset aggradation (e.g. Prince & Burgess, 2013: Fig. 10). Increased sediment delivery to the basin margin could be attributed to significant tectonic uplift in the Madagascan hinterlands to the east, climate change or an interplay between these two factors. Mountains in eastern Madagascar possibly formed during Early Cretaceous as a result of sedimentary loading within the Mahajanga and Morondava basins (Seward *et al.*, 2004; Emmel *et al.*, 2012) and due to regional stress changes along the evolving plate boundaries between India, Australia, Antarctica and Madagascar, and resulting transpression between India and Madagascar (Luger *et al.*, 1994; Giese *et al.*, 2012; Gaina *et al.*, 2013, 2015). In addition to a changing plate circuit, an expansion of the southern arid belt (Chumakov *et al.*, 1995) coupled with the northward migration of Madagascar into the subtropical zone (Fig. 11), could have decreased vegetation cover and increased seasonality, resulting in an increase in sediment supply. This was suggested by Rogers (2005) for younger Cretaceous strata and indicates that high supply and a seasonal/dry climate possibly prevailed during much of the Late Cretaceous in Madagascar. A reset of the progradational system occurred across the transgressive (SS5) surface (Fig. 4). This marked the transition from maximum progradation and lowstand (SP4) to pronounced aggradation (SP5).

The evolution of the margin and the increase in siliciclastic input from Albian to Turonian appears to have had a significant influence on deeper parts of the Mahajanga Basin. The prograding margin and the preservation of large-scale clinoforms suggest that a large amount of sediment was stored on the previously established Middle Jurassic carbonate shelf and possibly resulted in starved conditions further downdip. As progradation continued, the Middle Jurassic paleoshelf was bypassed and a significant amount of sediment was deposited rapidly in the deep basin. This rapid loading of sediments likely triggered halokinetic movement in the basin, forming large allochthonous and autochthonous salt structures (Tari *et al.*, 2004; Fig. 8).

The lack of significant unconformities described in outcrop by Besairie (1972) in the Albian to Turonian strata is puzzling. The subsurface data illustrate a margin that prograded for *ca*. 70 km, with earlier clinoforms exposed landward of the evolving shelf margin. This suggests that a significant time gap should be present between the exposed clinoforms (C1 through C3; i.e. *ca*. 113 to *ca*. 107 Ma) and the overlying transgressive deposits of SP5 (*ca*. 92 Ma; Figs 4 and 5). This time gap should be time equivalent to the deposition of C4 through C10

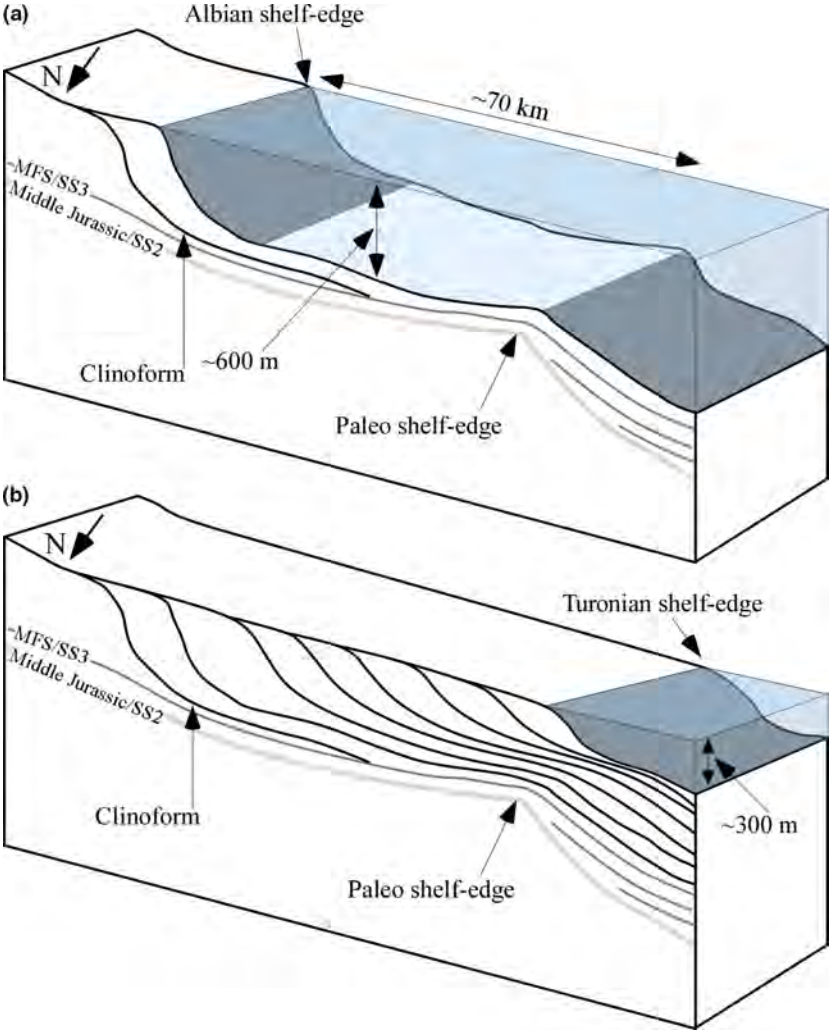

Fig. 10. Schematic box diagram displaying the evolution of the western margin of Madagascar from Albian (a) to Turonian (b). Diagrams show the clear reduction in clinoform size as progradation occurs and bathymetric relief is reduced.

clinoforms (Fig. 4c), a substantial time gap not noticed in previous studies (e.g. Besairie, 1972). Such a time gap, however, is present in the Morondava Basin to the south and is interpreted to have resulted from significant tectonic uplift and basin axis tilting due to the fragmentation of eastern Gondwana (Luger *et al.*, 1994; Giese *et al.*, 2012). Interestingly, a time gap was recognized by Besairie (1972) on outcrop in Upper Jurassic–Early Cretaceous strata, but this unconformity is not evident on the 2D profiles (Fig. 4). A possibility is that the shales above the Middle Jurassic carbonate platform are condensed, representing more time than previous studies suggest (e.g. Besairie, 1972). These observations require further detailed analysis and field examination.

The morphological changes in clinoforms along depositional strike from tangential oblique to ramp-like away from the 2D profile in Figure 4 are interesting. Similar lateral variations in other basins have been attributed to changes in sediment supply along strike, changes in basin physiography or changes in accommodation (e.g. Kertznus & Kneller, 2009; Henriksen *et al.*, 2011; Anell & Midtkandal, 2017). The highly progradational margin along the interpreted 2D profile could also indicate a point source linked to deltaic input (e.g. Olariu & Steel, 2009) located close to the displayed 2D profile in Figure 4. This is in agreement with the field observations of Besairie (1972), who saw up to 600 m of Aptian–Albian sandstones near the location of the 2D profile (Figs 2 and 4).

The documented decrease in clinoform height and slope length along depositional dip suggests a progressive decrease in accommodation as bathymetric relief was filled during progradation (Fig. 9). The flat bathymetry inherited from the drowned Middle Jurassic carbonate platform appears to have had an influence on clinoform geometries. This interpretation suggests that accommodation decreased progressively as topsets, foresets and bottomsets accumulated. Numerical models indicate that clinoform height and slope length are significantly influenced by the presence of a flat bathymetry and that a margin will become highly progradational as accommodation is decreased (e.g. Pirmez *et al.*, 1998). Moreover, Pirmez

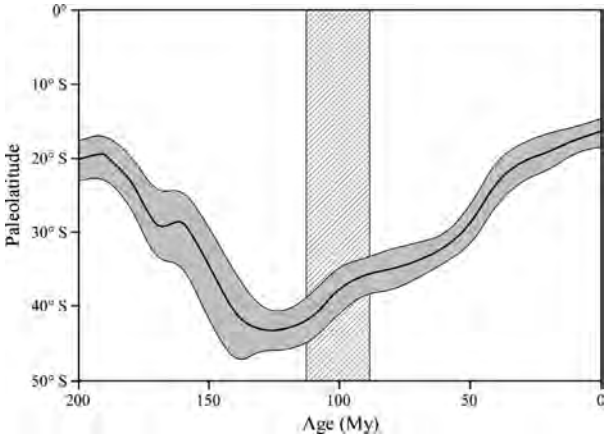

Fig. 11. Paleolatitude migration of Madagascar from 200 Ma to its present position at *ca*. 16.4° S. Notice the slow northward migration of Madagascar from *ca*. 130 Ma to present. Grey envelope is the 95% confidence interval on paleolatitude and hachured area highlights the approximate time during which progradation of the siliciclastic margin occurred. Paleolatitude from van Hinsbergen *et al.* (2015).

et al. (1998) modelled a constant slope gradient during a highly progradational phase by maintaining a constant sediment supply. This relationship could indicate that sediment supply in Madagascar was high but relatively constant throughout progradation.

Finally, the geometrical characteristics of the Mahajanga Basin clinoforms, when compared with other well-studied post-rift passive margin and foreland basin clinoforms, reveal similar attributes (Table 1). The progradational rate calculated for the clinoforms, however, is significantly lower than other basin margin progradational rates (Table 1). This discrepancy is probably caused by the lack of chronological constraints within individual clinoforms. A plausible scenario is that progradation of the margin occurred at a much faster pace, but was later controlled by the inherited Middle Jurassic shelf edge. Stratigraphic forward models have shown a relationship between inherited shelf edges and the basinward extent of younger progradational systems (e.g. Burgess & Steel, 2008). These inherited shelf edges can increase the gradient on which younger prograding systems advance, resulting in mass failure and deposition of mass transport complexes (MTCs) in deeper parts of the basin (e.g. Kertznus & Kneller, 2009). In the Mahajanga Basin, the basinward extent of the Albian–Turonian progradational phase and the location of the shelf-edge during C8–C10 seem to coincide with the position of the inherited shelf edge of the Middle Jurassic carbonate platform (Figs 4 and 6). A possibility is that progradation occurred much faster until the clinoforms reached the inherited Middle Jurassic shelf edge. The sudden increase in slope gradient beyond the Middle Jurassic shelf edge could induce failure and sediment bypass, hindering clinoform growth and progradation. It is possible that progradation ceased at this time. This would suggest that sediment bypass and slope failure continued for a significant amount of time until the margin was flooded during Turonian times. The increase in sediment bypass and resulting MTCs, deposited in the deep basin, would have resulted in rapid sediment deposition in the basin, possibly triggering salt movement (Tari *et al.*, 2004; Fig. 8). Confirmation of these observations would require field examination and better chronological constraints within individual clinoforms.

CONCLUSIONS

Quantification of clinoform geometries and trajectory analysis in the Mahajanga Basin, northwestern Madagascar, provides a case study of shelf-margin accretion. This study also illustrates the integration of outcrop geology along the surface of onshore 2D profiles to provide direct geologic calibration to a seismic interpretation. The results suggest that two variables influenced clinoform geometries and progradational patterns. First, the flat palaeobathymetry inherited from the underlying Middle Jurassic carbonate platform before the onset of progradation is interpreted as a significant control on subsequent clinoform geometries. As clinoform progradation progressed, bottomsets filled the available space and clinoform height was significantly reduced. Second, tectonically driven increase in sediment supply, perhaps coupled with a climatically driven spike in erosion and sediment delivery, is interpreted as the cause of the highly progradational margin with a flat shelf-edge trajectory. Progradation occurred during global sea-level maxima and differs from other Cenomanian–Turonian sedimentary records displaying periods of maximum transgression. This study shows that the architectural development of continental margins can be substantially controlled by inherited bathymetry, high sediment supply and sea level, and it provides a unique example from a previously understudied basin.

ACKNOWLEDGEMENTS

We thank ConocoPhillips for allowing publication of this work. We thank OMNIS and CGG MCNV (GeoSpec) for permission to publish the seismic data. We also like to thank the Global New Ventures and Technology groups in ConocoPhillips, especially Soeren Holm, Yves Chevalier, Carla Phelps, Johanna Moutoux and Mike Northrop. Their help and support substantially improved the quality of this work. Tor O. Sømme, Chris Elders, Editor Atle Rotevatn and one anonymous reviewer offered insightful comments that

significantly improved the quality of this manuscript. We also thank Editor Cynthia Ebinger, Carmen Gaina, Zhixin Li and Peter Burgess for providing useful comments on an earlier version of this manuscript. Thanks to G. Tari for providing permission to use a geoseismic profile and R. Tucker for providing the geologic map of Madagascar; both were essential for this work. RRR acknowledges funding from NSF (EAR-1664432).

REFERENCES

Abramovich, S., Keller, G., Adatte, T., Stinnesbeck, W., Hottinger, L., Stueben, D., Berner, Z., Ramanivosoa, B. & Randriamanantenasoa, A. (2002) Age and paleoenvironment of the Maastrichtian to Paleocene of the Mahajanga Basin, Madagascar: a multidisciplinary approach. *Mar. Micropaleontol.*, **47**, 17–70.

Anell, I. & Midtkandal, I. (2017) The quantificable clinothem – types, shapes and geometric relationships in the Plio-Pleistocene Giant Foresets Formation, Taranaki Basin, New Zealand. *Basin Res.*, **29**, 277–297.

Bardintzeff, J.-M., Liégeois, J.P., Bonin, B., Bellon, H. & Rasamimanana, G. (2010) Madagascar volcanic provinces linked to the Gondwana break-up: geochemical and isotopic evidences for contrasting mantle sources. *Gondwana Res.*, **18**, 295–314.

Besairie, H. (1972) Géologie de Madagascar. I. Les Terrains Sédimentaires. Annales Géologiques de Madagascar 35.

Burgess, P.M. & Prince, G.D. (2015) Non-unique stratal geometries: implications for sequence stratigraphic interpretations. *Basin Res.*, **27**, 351–365.

Burgess, P.M. & Steel, R. (2008) Stratigraphic forward modeling of basin-margin clinoform systems: implications for controls on topset and shelf width and timing of formation of shelf-edge deltas. In: *Recent Advances in Models of Siliciclastic Shallow-Marine Stratigraphy* (Ed. by Hampson G.J., Steel R.J., Burgess P.M. & Dalrymple R.W.) *SEPM Spec. Publ.*, **90**, 35–45.

Carvajal, C.R. & Steel, R.J. (2006) Thick turbidite successions from supply-dominated shelves during sea-level highstand. *Geology*, **34**, 665–668.

Catuneanu, O. (2002) Sequence stratigraphy of clastic systems: concepts, merits, and pitfalls. *J. Afr. Earth Sc.*, **35**, 1–43.

Chumakov, N.M., Zharkov, M.A., Herman, A.B., Doludenko, M.P., Kalandadze, N.N., Lebedev, E.A., Ponomarenko, A.G. & Rautian, A.S. (1995) Climate belts of the Mid-Cretaceous time. *Stratigr. Geol. Correl.*, **3**, 241–260.

Cucciniello, C., Melluso, L., Jourdan, F., Mahoney, J.J., Meisel, T. & Morra, V. (2013) ^{40}Ar-^{39}Ar ages and isotope geochemistry of Cretaceous basalts in northern Madagascar: refining eruption ages, extent of crustal contamination and parental magmas in a flood basalt province. *Geol. Mag.*, **150**, 1–17.

Eagles, G. & König, M. (2008) A model of plate kinematics in Gondwana breakup. *Geophys. J. Int.*, **173**, 703–717.

Emmel, B., Boger, S.D., Jacobs, J. & Daszinnies, M.C. (2012) Maturity of central Madagascar's landscape — Low-temperature thermochronological constraints. *Gondwana Res.*, **21**, 704–713.

Gaina, C., Torsvik, T.H., van Hinsbergen, D.J.J., Medvedev, S., Werner, S.C. & Labails, C. (2013) The African Plate: a history of oceanic crust accretion and subduction since the Jurassic. *Tectonophysics*, **604**, 4–25.

Gaina, C., van Hinsbergen, D.J.J. & Spakman, W. (2015) Tectonic interactions between India and Arabia since the Jurassic reconstructed from marine geophysics, ophiolite geology, and seismic tomography. *Tectonics*, **34**, 875–906.

Geiger, M., Clark, D.N. & Mette, W. (2004) Reappraisal of the timing of the breakup of Gondwana based on sedimentological and seismic evidence from the Morondava Basin, Madagascar. *J. Afr. Earth Sc.*, **38**, 363–381.

Gibbons, A.D., Whittaker, J.M. & Muller, R.D. (2013) The breakup of East Gondwana: assimilating constraints from Cretaceous ocean basins around India into the best-fit tectonic model. *J. Geophys. Res.*, **118**, 1–15.

Giese, J., Seward, D. & Schreurs, G. (2012) Low-temperature evolution of the Morondava rift basin shoulder in western Madagascar: an apatite fission track study. *Tectonics*, **31**. TC2009.

Goodbreed, S.L. & Kuehl, S.A. (2000) The significance of large sediment supply, active tectonism, and eustasy on margin sequence development: late quaternary stratigraphy and evolution of the Ganges-Brahmaputra delta. *Sed. Geol.*, **133**, 227–248.

Gradstein, F.M., Ogg, J.G. & Smith, A.G. (2004) *A Geologic Time Scale 2004*. pp. 589. Cambridge University Press, New York.

Henriksen, S., Helland-Hansen, W. & Bullimore, S. (2011) Relationships between shelf-edge trajectories and sediment dispersal along depositional dip and strike: a different approach to sequence stratigraphy. *Basin Res.*, **23**, 3–21.

Helland-Hansen, W. & Hampson, G.J. (2009) Trajectory analysis: concepts and applications. *Basin Res.*, **21**, 454–483.

Helland-Hansen, W. & Martinsen, O.J. (1996) Shoreline trajectories and sequences; description of variable depositional-dip scenarios. *J. Sediment. Res.*, **66**, 670–688.

van Hinsbergen, D., de Groot, L.V., van Schaik, S.J., Spakman, W., Bijl, P.K., Sluijs, A., Langereis, C.G. & Brinkhuis, H. (2015) A paleolatitude calculator for paleoclimate studies. *PLoS ONE*, **10**, 1–21.

Hubbard, S.M., Fildani, A., Romans, B.W., Colvault, J.A. & McHargue, T.R. (2010) High-relief slope clinoform development: insights from outcrop, Magallanes Basin, Chile. *J. Sediment. Res.*, **80**, 357–375.

Johannessen, E.P. & Steel, R.J. (2005) Shelf-margin clinoforms and prediction of deepwater sands. *Basin Res.*, **17**, 521–550.

Kertznus, V. & Kneller, B. (2009) Clinoform quantification for assessing the effects of external forcing on continental margin development. *Basin Res.*, **21**, 738–758.

Leinweber, V.T. & Jokat, W. (2012) The Jurassic history of the Africa-Antarctica corridor — new constraints from magnetic data on the conjugate continental margins. *Tectonophysics*, **530–531**, 87–101.

Luger, P., Gröschke, M., Bussman, M., Dina, A., Mette, W., Uhmann, A. & Kallenbach, H. (1994) Comparison of the

Jurassic and Cretaceous sedimentary cycles of Somalia and Madagascar: implications for the Gondwana breakup. *Geol. Rundsch.*, **83**, 711–727.

Melluso, L., Morra, V., Brotzu, P. & Mahoney, J.J. (2001) The cretaceous igneous province of madagascar: geochemistry and petrogenesis of lavas and dykes from the central–western sector. *J. Petrol.*, **42**, 1249–1278.

Miller, K.G., Kominz, M.A., Browning, J.V., Wright, J.D., Mountain, G.S., Katz, M.E., Sugarman, P.J., Cramer, B.S., Christie-Blick, N. & Pekar, S.F. (2005) The phanerozoic record of global sea-level change. *Science*, **310**, 1293–1298.

Mitchum, R.M., Vail, P.R. & Sangree, J.B. (1977) Seismic stratigraphy and global changes of sea level, part 6: stratigraphic interpretation of seismic reflection patterns in depositional sequences. In: *Seismic Stratigraphy - Applications to Hydrocarbon Exploration* (Ed. by C.E. Payton), AAPG, Tulsa.

Muto, T. & Steel, R.J. (2002) In defence of shelf-edge delta development during falling and lowstand of relative sea level. *J. Geol.*, **110**, 421–436.

Nguyen, L.C., Hall, S.A., Bird, D.E. & Ball, P.J. (2016) Reconstruction of the East Africa and Antarctica continental margins. *J. Geophys. Res. Solid Earth*, **121**, https://doi.org/10.1002/2015JB012776.

Olariu, C. & Steel, R.J. (2009) Influence of point-source sediment-supply on modern shelf-slope morphology: implications for interpretation of ancient shelf margins. *Basin Res.*, **21**, 484–501.

Papini, M. & Benvenuti, M. (1998) Lithostratigraphy, sedimentology, and facies architecture of the Late Cretaceous succession in the central Mahajanga Basin, Madagascar. *J. Afr. Earth Sc.*, **26**, 229–247.

Papini, M. & Benvenuti, M. (2008) The Toarcian-Bathonian succession of the Antsiranana Basin (NW Madagascar): facies analysis and tectono-sedimentary history in the development of the East Africa-Madagascar conjugate margins. *J. Afr. Earth Sc.*, **51**, 21–38.

Patruno, S., Hampson, G.J. & Jackson, C.A.L. (2015) Quantitative characterisation of deltaic and subaqueous clinoforms. *Earth Sci. Rev.*, **142**, 79–119.

Pirmez, C., Pratson, L.F. & Steckler, M.S. (1998) Clinoform development by advection-diffusion of suspended sediment: modeling and comparison to natural systems. *J. Geophys. Res. Solid Earth*, **103**, 24141–24157.

Pomar, L. (2001) Types of carbonate platforms: a genetic approach. *Basin Res.*, **13**, 313–334.

Posamentier, H.W. & Vail, P.R. (1988) Eustatic controls on clastic deposition II - sequence and systems tract models. In: *Sea Level Changes: An Integrated Approach*. (Ed. by Wilgus C.K., Hastings B.S., Kendall C.G., Posamentier H.W., Ross C.A. & Van Wagoner J.C.), *SEPM Spec. Publ.*, **42**, 125–154.

Posamentier, H.W., Jervey, M.T. & Vail, P.R. (1988) Eustatic controls on clastic deposition I - conceptual framework. In: *Sea Level Changes: An Integrated Approach* (Ed. by Wilgus C.K., Hastings B.S., Kendall C.G., Posamentier H.W., Ross C.A. & Van Wagoner J.C.) *SEPM Spec. Publ.*, **42**, 110–124.

Pratt, M.J., Wysession, M.E., Aleqabi, G., Wiens, D.A., Nyblade, A.A., Shore, P., Rambolamanana, G. & Andriampenomanana, F. (2016) Shear velocity structure of the crust and upper mantle of Madagascar derived from surface wave tomography. *Earth Planet. Sci. Lett.*, **458**, 405–417.

Prince, G.D. & Burgess, P.M. (2013) Numerical modeling of falling-stage topset aggradation: implications for distinguishing between forced and unforced regressions in the geological record. *J. Sediment. Res.*, **83**, 767–781.

Reeves, C.V., Teasdale, J.P. & Mahanjane, E.S. (2016) Insight into the Eastern Margin of Africa from a new tectonic model of the Indian Ocean. In: *Transform Margins: Development, Controls, and Petroleum Systems* (Ed. by Nemcok M., Rubar S., Sinha S.T., Hermeston S.A. & Lendenyiova L.) *Geol. Soc. Spec. Pub.*, **431**, 299–322.

Rich, J.L. (1951) Three critical environments of deposition and criteria for recognition of rocks deposited in each of them. *Geol. Soc. Am. Bull.*, **62**, 1–20.

Roberts, G.G., Paul, J.D., White, N. & Winterbourne, J. (2012) Temporal and spatial evolution of dynamic support from river profiles: a framework for Madagascar. *Geochem. Geophys. Geosyst.*, **13**. Q04004

Rogers, R.R. (2005) Fine-grained debris flows and extraordinary vertebrate burials in the Late Cretaceous of Madagascar. *Geology*, **33**, 297–300.

Rogers, R.R., Hartman, J.H. & Krause, D.W. (2000) Stratigraphic analysis of Upper Cretaceous rocks in the Mahajanga Basin, northwestern Madagascar: implications for ancient and modern faunas. *J. Geol.*, **108**, 275–301.

Rogers, R.R., Krause, D.W. & Rogers, K.C. (2003) Cannibalism in the Madagascan dinosaur *Majungatholus atopus*. *Nature*, **422**, 515–518.

Rogers, R.R., Krause, D.W., Rogers, K.C., Rasoamiaramanana, A.H. & Rahantarisoa, L. (2007) Paleoenvironment and paleoecology of *Majungasaurus crenatissimus* (Theropoda: Abelisauridae) from the late Cretaceous of Madagascar. *J. Vertebr. Paleontol.*, **27**, 21–31.

Rogers, R.R., Krause, D.W., Kast, S.C., Mashall, M.S., Rahantarisoa, L., Robins, C.R. & Setich, J.J.W. (2013) A new, richly fossiliferous member comprised of tidal deposits in the Upper Cretaceous Maevarano Formation, northwestern Madagascar. *Cretac. Res.*, **44**, 12–29.

Roig, J.Y., Tucker, R.D., Peters, S.G., Delor, C. & Theveniaut, H. (2012) Carte Geologique de la Republique de Madagascar.

Schandelmeier, H., Bremer, F. & Holl, H.G. (2004) Kinematic evolution of the Morondava rift basin of SW Madagascar—from wrench tectonics to normal extension. *J. Afr. Earth Sc.*, **38**, 321–330.

Schlanger, S.O., Arthur, M.A., Jenkyns, H.C. & Scholle, P.A. (1987) The Cenomanian-Turonian Oceanic Anoxic Event, I. Stratigraphy and distribution of organic carbon-rich beds and the marine δ13C excursion. *Geol. Soc. Spec. Publ.*, **26**, 371–399.

Seward, D., Grujic, D. & Schreurs, G. (2004) An insight into the breakup of Gondwana: identifying events through low-temperature thermochronology from the basement rocks of Madagascar. *Tectonics*, **23**, 1–20.

Steckler, M.S., Mountain, G.S., Miller, K.G. & Christie-Blick, N. (1999) Reconstruction of Tertiary progradation and

clinoform development on the New Jersey passive margin by 2-D backstripping. *Mar. Geol.*, **154**, 399–420.

Steel, R.J. & Olsen, T. (2002) Clinoforms, clinoform trajectories and deepwater sands. In: *Sequence Stratigraphic Models for Exploration and Production: Evolving Methodology, Emerging Models, and Application Histories* (Ed. by Armentrout J.M. & Rosen N.C) *GCS-SEPM Spec. Publ.*, pp. 367–381.

Storey, M., Mahoney, J.J. & Saunders, A.D. (1997) Cretaceous basalts in Madagascar and the transition between plume and continental lithosphere mantle sourced. In: *Large Igneous Provinces: Continental, Oceanic and Planetary Flood Volcanism* (Ed. by Mahoney J.J. & Coffin M.F.) *Geophys. Monog., Amer. Geophys. Union* **100**, 95–122.

Tari, G., Coterill, K., Molnar, J., Valasek, D., Walters, G. & Alvarez, Y. (2004) Salt tectonics and sedimentation in the offshore Majunga Basin, Madagascar. In: *Salt-Sediment Interactions and Hydrocarbon Prospectivity: Concepts, Applications, and Case Studies for the 21st Century* (Ed. by P.J. Post, D.L. Olson, K.T. Lyons, S.L. Palmes, P.F. Harrison, N.C. Rosen), pp. 614–639. GCSSEPM Foundation, Houston, TX.

Torsvik, T.H., Tucker, R.D., Ashwal, L.D., Carter, L.M., Jamtveit, B., Vidyadharan, K.T. & Venkataramana, P. (2000) Late Cretaceous India-Madagascar fit and timing of break-up related magmatism. *Terra Nova*, **12**, 220–224.

Wild, R., Flint, S.S. & Hodgson, D.M. (2009) Stratigraphic evolution of the upper slope and shelf edge in the Karoo Basin, South Africa. *Basin Res.*, **21**, 502–527.

Vail, P.R. & Mitchum, R.M. (1977) Seismic stratigraphy and global changes of sea level: part 1. In: *Seismic Stratigraphy - Applications to Hydrocarbon Exploration* (Ed. by C.E. Payton), AAPG, Tulsa.

Manuscript received 24 July 2017; In revised form 18 October 2017; Manuscript accepted 19 October 2017.